
Philosophical Magazine Letters
Publication details, including instructions for authors and subscription information:
http://www.tandfonline.com/loi/tphl20

# Interplay between deformation twins and basal stacking faults enriched with Zn/Y in $Mg_{97}Zn_1Y_2$ alloy

X.H. Shao[a], Z.Q. Yang[a] & X.L. Ma[a]
[a] Shenyang National Laboratory for Materials Science, Institute of Metal Research, Chinese Academy of Sciences, Shenyang 110016, China
Published online: 14 Mar 2014.

To cite this article: X.H. Shao, Z.Q. Yang & X.L. Ma (2014) Interplay between deformation twins and basal stacking faults enriched with Zn/Y in $Mg_{97}Zn_1Y_2$ alloy, Philosophical Magazine Letters, 94:3, 150-156, DOI: 10.1080/09500839.2014.885123

To link to this article: http://dx.doi.org/10.1080/09500839.2014.885123

*Philosophical Magazine Letters*, 2014
Vol. 94, No. 3, 150–156, http://dx.doi.org/10.1080/09500839.2014.885123



# Interplay between $\{1\,0\,\bar{1}\,2\}$ deformation twins and basal stacking faults enriched with Zn/Y in $Mg_{97}Zn_1Y_2$ alloy

X.H. Shao*, Z.Q. Yang and X.L. Ma

*Shenyang National Laboratory for Materials Science, Institute of Metal Research, Chinese Academy of Sciences, Shenyang 110016, China*

(*Received 30 August 2013; accepted 31 December 2013*)

Basal stacking faults (SFs) enriched with Zn/Y are identified in an $Mg_{97}Zn_1Y_2$ alloy, and the interaction between SFs and $\{1\,0\,\bar{1}\,2\}$ deformation twins (DTs) is characterized at the atomic scale by means of high-resolution transmission electron microscopy. Such an interaction results in deviations of twin angle from its theoretical value and twin boundary (TB) from its $(1\,0\,\bar{1}\,2)$ habit plane. In addition, the DT-SF reaction not only leads to the TB with terraces along basal planes, but also makes the TB broaden with severe distortion. The role of long-period stacking ordered lamellae in propagation of DTs is also clarified based on the atomic-scale high-resolution images.

**Keywords:** deformation twin; stacking fault; habit plane; Mg alloy; HAADF-STEM



## 1. Introduction

Mechanical twinning is an important deformation mechanism in Mg alloys, especially at low temperatures or at high strain rates, since slip systems are quite limited in the hexagonal close-packed (HCP) lattice structure [1,2]. The mechanical properties of Mg alloys can be significantly affected by twins [3–6]. For example, the unidirectional nature of twinning can cause high levels of mechanical asymmetry in wrought Mg alloys produced after the thermo-mechanical processing [7,8]. In addition, twin boundaries (TBs) were found to be the preferred sites for the initiation of cracks, which may lead to premature failure [9–12]. If the nucleation and propagation of deformation twins (DTs) can be effectively inhibited, it might be possible to suppress the premature local cracking in the Mg alloys. The formation and growth of DTs and their interaction with the precipitates, and their effect on the mechanical properties of Mg alloys are thus of particular interest [13,14].

Recently, Mg–Zn–Y alloy containing long-period stacking ordered (LPSO) phase has attracted considerable attention due to its excellent mechanical properties [15–19]. One of the reasons is that the LPSO phase or the stacking faults (SFs) with a high density prevent the growth of the $\{1\,0\,\bar{1}\,2\}$ DT [18,20]. However, the reaction mechanism between the DTs and SFs or the LPSO phase in Mg alloys has not been well understood. In this work, we characterized the propagation of $\{1\,0\,\bar{1}\,2\}$ DTs and their

*Corresponding author. Email: xhshao@imr.ac.cn

interactions with the basal SFs enriched with Zn/Y and with thin LPSO lamella in the $Mg_{97}Zn_1Y_2$ (at.%) alloy at the atomic level via transmission electron microscopy (TEM). And we proposed the possible mechanisms based on the experimental observations. This study may lead to a better understanding of the deformation mechanism in Mg alloys containing profuse SFs enriched with solute elements.

## 2. Experimental procedure

$Mg_{97}Zn_1Y_2$ (at.%) alloy was prepared from a high purity Mg, Zn and Mg-25Y (wt.%) master alloy by high-frequency induction melting in a graphite crucible at approximately 1023 K under an argon atmosphere. Specimens with dimensions of $4 \times 4 \times 8\ mm^3$ were cut from ingots by electrical discharge machining. Compression experiments were carried out at 373 K under a strain rate of $1.0 \times 10^{-3}\ s^{-1}$ in a Gleeble-1500 thermal simulation machine. Prior to the compression, the specimens were conductively heated to 373 K at a heating rate of $5\ K\ s^{-1}$ and held for 180 s for equilibration. TEM thin foil samples were prepared by the conventional ion-milling method. A Tecnai $G^2$ F30 TEM, operated at 300 kV and equipped with a high angle annual dark-field detector, was used for microstructure characterization and analysis.

## 3. Results and discussion

Figure 1 is a representative TEM image, showing the morphology of the DT in the $Mg_{97}Zn_1Y_2$ alloy after compression. As demonstrated by the electron diffraction pattern (EDP), shown as an inset, the needle-like domain is a $\{1\,0\,\bar{1}\,2\}$ DT. The misorientation between the matrix and the twin is about 81°, ~5° lower than the theoretical angle/axis

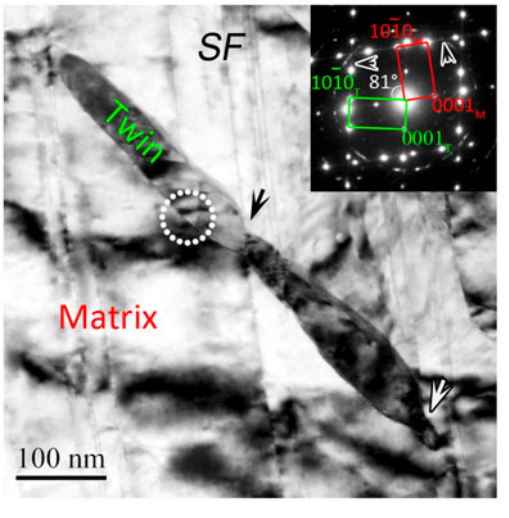


Figure 1. (colour online). TEM analysis of a typical $\{1\,0\,\bar{1}\,2\}$ twin in an Mg–Zn–Y alloy deformed at 373 K and at a strain rate of $1.0 \times 10^{-3}$/s. The inset is the corresponding electronic diffraction pattern, showing the misorientation between the twin and the matrix is about 81°.

pair of about 86° [21]. It was also found, as denoted by arrows in Figure 1, the DT shrinks and is deflected where it intersects with SFs, unambiguously indicating the strong interactions between the DT and SFs.

Figure 2a shows a high-resolution-TEM (HRTEM) image of the $\{1\,0\,\bar{1}\,2\}$ TB penetrating an SF. The misorientation between the basal planes of matrix and the twin is approximately 84°. Obviously, the TB is curved and deviated from the $(1\,0\,\bar{1}\,2)$ habit plane. A 4-nm-wide waved ledge with severely distorted lattice contrast was observed along the TB (the region marked by dashed lines in Figure 2a), significantly different from the relatively sharp TBs in other Mg alloys [22,23]. As shown in the magnified image (inset in Figure 2a), an intrinsic SF (ISF: stacking sequence …*ABCBCB*…, first *C* plane denoted by an arrow) emits from the TB. This ISF is likely formed due to the dissociation of the $a+c$ dislocation [24], without an obvious Zn/Y aggregation as

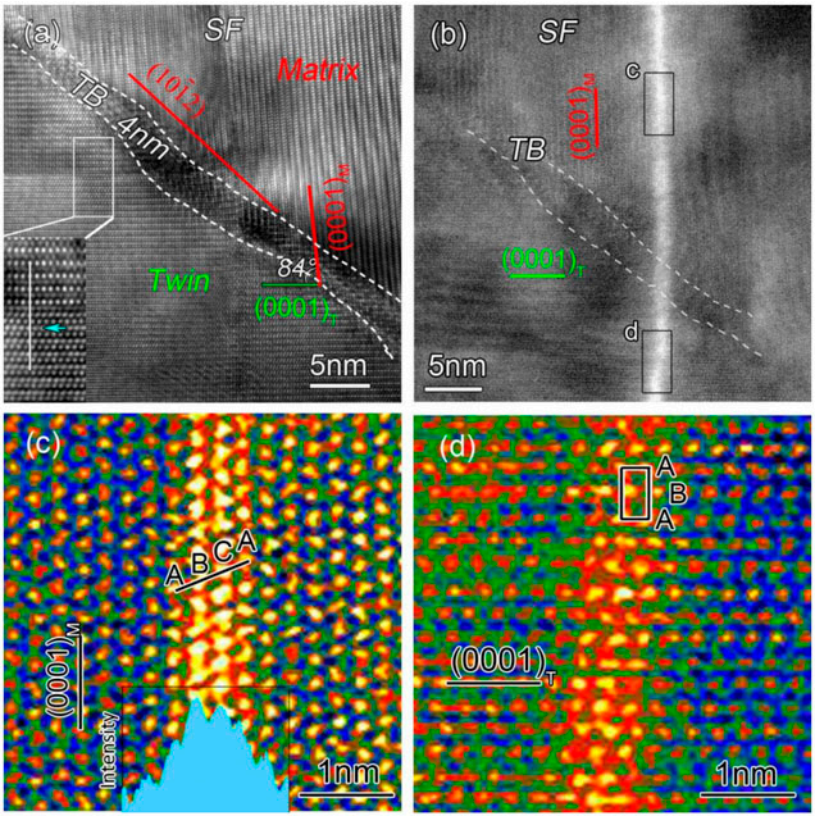


Figure 2. (colour online). (a) HRTEM image of a $\{1\,0\,\bar{1}\,2\}$ TB penetrating SFs in the sample. The inset is the magnified image of region denoted by the rectangle, showing the atomic stacking sequence changes from …*ABAB*… to …*ABCBCB*…, where c plane is marked by an arrow, indicating an intrinsic SF. (b) Corresponding HR-STEM image of Figure 2a. The TB is marked by dashed lines in (a) and (b). (c) and (d) HR-STEM image of the distribution of Zn/Y before and after TB penetrating the SF. The inset in (c) is the line profile crossing the SF, demonstrating higher Zn/Y segregation in the middle planes *B* and *C*.

suggested by the Z-contrast image (Figure 2b). The high-resolution Z-contrast images of regions *c* and *d* in figure 2b are further presented in Figures 2c and d, respectively. The stacking sequence of the SF in Figure 2c is *ABCA*, and the two middle layers are brighter due to higher concentration of Zn and/or Y, compared with the adjacent layers, as shown by the line intensity inserted. Figure 2d demonstrates that the Zn/Y atoms, denoted by brighter spots, segregate in 3–4 adjacent prismatic planes in the DT, as indicated by the square showing a unit cell of the HCP structure. Figure 2c and d suggests that a reaction must occur to convert the original *ABCA* fault structure to the *ABAB* stacking upon twinning, in order to form the observed HCP stacking sequence in the twin, according to the $\{1\,0\,\bar{1}\,2\}$ twinning mechanism [25]. Such a reaction can be triggered by the glide of a Shockley partial dislocation in the basal plane, which is similar to the de-twinning process in face-centred cubic metals.

The microstructure of a DT crossing SFs and bypassing a 12-nm-thick LPSO plate is demonstrated in Figure 3. The TEM and STEM images in Figure 3a and b indicate that the TB becomes rather wavy at the intersection of the TB with the thin LPSO plate, such as at the rectangular area *d*. Figure 3c is the corresponding HRTEM image of the area marked by *c* rectangle in Figure 3a. It shows the $\{1\,0\,\bar{1}\,2\}$ DT cut through the three units of SFs, separating from each other about 10 and 6 nm, respectively. The TB obviously deflects from the original direction and forms terraces (marked by open arrows in Figure 3c), accompanied by a blurred complex ledge of about 20 nm in thickness (marked by the dashed lines). Figure 3d is a HRTEM image of the rectangular area *d* in Figure 3a, presenting the atomic structure of the DT intersecting into a 12-nm-thick LPSO plate. Severe local lattice bending of basal planes is observed in the LPSO plate with a thickness of about 5 nm, as indicated by white arrows, and a lattice distortion is about 6°. It demonstrates that the LPSO plate undergoes plastic deformation to accommodate the matrix twinning. However, the original LPSO tip is apparently rotated into

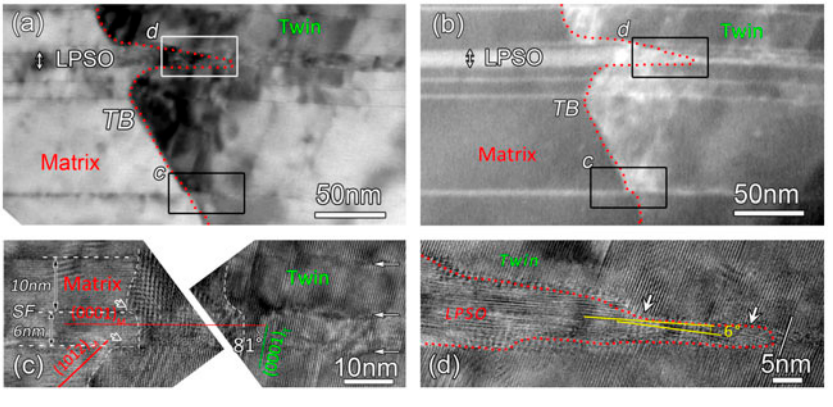


Figure 3. (colour online). (a) A TEM image and (b) a low-magnification STEM image showing $\{1\,0\,\bar{1}\,2\}$ TB running into SFs and thin LPSO plate in the sample, respectively. (c) The corresponding HRTEM images of the region marked by rectangle *c* in Figure 3a and b, showing the TB cut through the three units of SFs. (d) The corresponding HRTEM images of the area marked by rectangle *d* in Figure 3a and b, demonstrating the TB bypasses the 12 nm wide LPSO lamella.

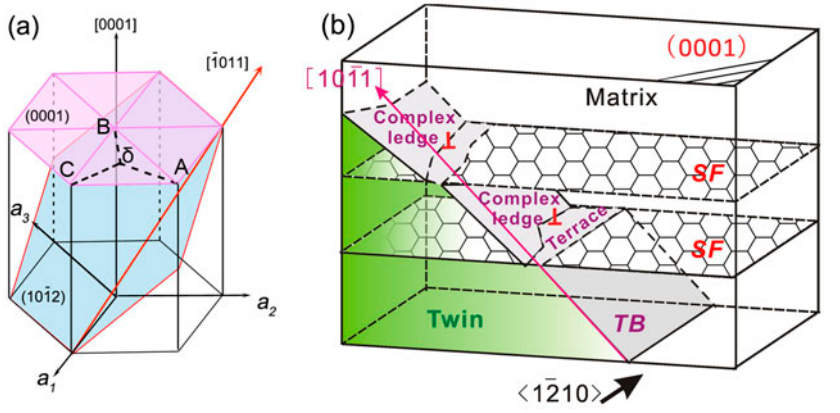


Figure 4. (colour online). (a) Crystallographic structures of Mg lattice structures. Pink and blue surfaces represent basal and twinning planes, and red vector denotes twinning direction. (b) Schematic drawing of a configuration of interaction between SFs and DT. The matrix-twin interfaces are represented as grey regions, and incident beam direction and twinning direction are also shown by black and red arrows, respectively.

the twin orientation, whose basal planes are denoted by a white line in DT (figure 3d). Thus, the DT can twin the LPSO slice thinner than ~5 nm, that is about one unit of the 18R-LPSO phase (4.68 nm), but it bypasses the 12-nm-thick LPSO plate under the current deformation situation.

The above results indicate that: (i) the twin angles deviate from the idea value while DT intersecting with the layers enriched with Zn/Y. (ii) TBs deflect from the habit plane, and the complex TB structure is closely associated with the strong reactions between the SFs and DTs. (iii) The LPSO plate with a critical thickness or a certain number of consecutive SFs could be expected to hinder the propagation of DTs.

Figure 4a illustrates a crystallographic structure of Mg, in which the (0 0 0 1) basal plane and the (1 0 $\bar{1}$ 2) twinning plane are coloured in pink and blue, respectively. The twin direction [1 0 $\bar{1}$ 1] is indicated by a red arrow. $A\delta$, $B\delta$ and $C\delta$ represent basal Shockley partials with Burgers of $\frac{1}{3}$[0 1 $\bar{1}$ 0], $\frac{1}{3}$[1 $\bar{1}$ 0 0] and $\frac{1}{3}$[1 0 $\bar{1}$ 0], respectively. The elementary twinning dislocation for the (1 0 $\bar{1}$ 2) twinning has a Burgers vector of 0.07[1 0 $\bar{1}$ 1] in Mg [26]. As indicated in Figure 2, the observed local lattice rearrangement in the SFs is equivalent to the glide of a basal Shockley partial along the original SF and the twinning shear, upon interacting with the (1 0 $\bar{1}$ 2) twinning. Considering both the basal Shockley partial and the twinning dislocation, the local shear vector is thus modified as $\mp X\delta + 0.07$[1 0 $\bar{1}$ 1] with $X$ for $A$, $B$ or $C$, at the intersections between SFs and the growing DT. Such a local shear redirects the propagation of the DT off its (1 0 $\bar{1}$ 2) habit plane, as shown schematically in Figure 4b, leading a terrace along basal planes. In addition, no edge-on structures were found in the modified TB along the viewing direction of [1 $\bar{2}$ 1 0] axis (Figure 4b). That is, the lattice overlap between the matrix and the twin makes the TB broaden with severe distortions in the HRTEM images (Figures 2 and 3), as well as the dislocations produced by the SF-DT reaction. Hence, the TB becomes wavy due to the terraces along basal plane, and it is extended

and blurred when viewed in $[1\,1\,\bar{2}\,0]$ directions owing to the overlap of matrix and twins.

It should be mentioned that TBs are observed to deflect from the habit plane when DTs intersect with precipitates or other domain structures in various materials. For example, the asymmetrical TBs in perovskite-based thin films is caused by the intersection of (1 1 1) twinning with the antiphase domain boundaries, and TBs are apart from the $(\bar{1}\,\bar{1}\,1)$ plane [27]. TB deflection from the habit plane in Mg-Al alloy is caused by the TB–dislocation interaction when DT bypasses the precipitates of comparable size [13]. The TBs with large deviations from the twinning plane in pure Co and pure Mg is explained by the shuffling mechanism [28], that is the shuffling does not have to be confined in the $\{1\,0\,\bar{1}\,2\}$ plane, and thus, the actual TBs might migrate far off the $\{1\,0\,\bar{1}\,2\}$ twinning plane during the twin growth [29]. However, the stepwise and wide TBs observed here (Figures 2 and 3) are obviously different from those wavy but sharp TBs reported in Mg or Mg alloys. The unique morphologies of TBs illustrated above should be closely related to the distinctive deformation mechanisms, owing to the difference in deformation methods (hand-made tension in Ref. [20]) or chemical compositions of materials (pure Mg in Ref. [29]).

The DT bypasses the LPSO plate (about 9 successive SFs) (Figure 3d), while it mechanically cuts through the two successive SFs extending from the LPSO plate. A previous study indicated that the critically resolved shear stress to move a basal Shockley partial was in the range of 26.5–60.4 MPa in a $Mg_{97}Zn_1Y_2$ alloy [24]. Therefore, the required resolved shear stress should be over 53 MPa, in order to obtain an HCP structure in the DT within the region containing two neighbouring SFs as shown in Figure 3. Considering that the yield stress of our $Mg_{97}Zn_1Y_2$ alloy is 90 MPa [18], the LPSO plate that can be sheared upon twinning should be composed of no more than three SFs, at the yielding point. This is consistent with our HRTEM results. As shown in Figure 3d, the thin LPSO phase or successive SFs, thicker than 5 nm, do not comply with the DT lattice. The profuse SFs could be introduced in Mg–Zn–Y alloy, because the addition of Y to Mg would significantly decrease the intrinsic SF energy of Mg alloys based on the experimental results and density functional theory [30]. Thus, strong SF/LPSO–DT reactions would be expected and effectively lower the necessary formation and/or propagation energy of DTs, and then hinder the deformation twinning to some extent. Consequently, this could suppress the preferred nucleation sites (i.e. TBs) for cracking and then benefit to its mechanical properties.

## 4. Conclusion

The crystallographic account of the unique propagation of $\{1\,0\,\bar{1}\,2\}$ DTs in $Mg_{97}Zn_1Y_2$ alloy is addressed based on high-resolution imaging. It is found that the interaction between the SFs enriched with Zn/Y and the DTs plays a significant role in the formation and growth of DTs. The DT–SF reactions not only make the twin angle deviate from the ideal value, but also change the lattice plane on which DT propagates. This study indicates that the SFs/LPSO phases in the Mg–Zn–Y alloy are critically important for improving the mechanical performance of Mg alloys through hindering DT propagation.

## Funding

The authors acknowledge the financial support from the National Basic Research Program of China [grant number 2009CB623705] and National Natural Science Foundation of China [grant number 51301177], [grant number 51171189] and NSF of Liaoning Province.

## References

[1] M. Barnett, Mater. Sci. Eng. A 464 (2007) p.1.
[2] M. Barnett, Mater. Sci. Eng. A 464 (2007) p.8.
[3] L. Jiang, J. Jonas, A. Luo, A. Sachdev and S. Godet, Scr. Mater. 54 (2006) p.771.
[4] M.R. Barnett, Z. Keshavarz, A.G. Beer and X. Ma, Acta Mater. 56 (2008) p.5.
[5] Y. Chino, K. Kimura and M. Mabuchi, Mater. Sci. Eng. A 486 (2008) p.481.
[6] H.J. Yang, S.M. Yin, C.X. Huang, Z.F. Zhang, S.D. Wu, S.X. Li and Y.D. Liu, Adv. Eng. Mater. 10 (2008) p.955.
[7] L. Jiang, J. Jonas, R. Mishra, A. Luo, A. Sachdev and S. Godet, Acta Mater. 55 (2007) p.3899.
[8] J. Jain, W. Poole, C. Sinclair and M. Gharghouri, Scr. Mater. 62 (2010) p.301.
[9] P. Cizek and M.R. Barnett, Scr. Mater. 59 (2008) p.959.
[10] J. Koike, Metall. Mater. Trans. A 36 (2005) p.1689.
[11] H. Somekawa, A. Singh and T. Mukai, Philos. Mag. Lett. 89 (2009) p.2.
[12] J. Koike, N. Fujiyama, D. Ando and Y. Sutou, Scr. Mater. 63 (2010) p.747.
[13] M.A. Gharghouri, G.C. Weatherly and J.D. Embury, Philos. Mag. A 78 (1998) p.1137.
[14] J.D. Robson, N. Stanford and M.R. Barnett, Acta Mater. 59 (2011) p.1945.
[15] Y. Kawamura, K. Hayashi, A. Inoue and T. Masumoto, Mater. Trans. 42 (2001) p.1172.
[16] M. Suzuki, T. Kimura, J. Koike and K. Maruyama, Scr. Mater. 48 (2003) p.997.
[17] M. Yamasaki, T. Anan, S. Yoshimoto and Y. Kawamura, Scr. Mater. 53 (2005) p.799.
[18] X.H. Shao, Z.Q. Yang and X.L. Ma, Acta Mater. 58 (2010) p.4760.
[19] X.H. Shao, H.J. Yang, J.T. De Hosson and X.L. Ma, Microsc. Microanal. 19 (2013) p.1575.
[20] M. Matsuda, S. Ii, Y. Kawamura, Y. Ikuhara and M. Nishida, Mater. Sci. Eng. A. 386 (2004) p.447.
[21] M. Nave and M. Barnett, Scr. Mater. 51 (2004) p.881.
[22] M. Myshlyaev, H. McQueen, A. Mwembela and E. Konopleva, Mater. Sci. Eng. A 337 (2002) p.121.
[23] J.T. Wang, D.L. Yin, J.Q. Liu, J. Tao, Y.L. Su and X. Zhao, Scr. Mater. 59 (2008) p.63.
[24] Z. Yang, M.F. Chisholm, G. Duscher, X. Ma and S.J. Pennycook, Acta Mater. 61 (2013) p.350.
[25] A. Serra and D.J. Bacon, Philos. Mag. A 73 (1996) p.333.
[26] J. Wang, I.J. Beyerlein and C.N. Tomé, Scr. Mater. 63 (2010) p.741.
[27] S.J. Zheng and X.L. Ma, Philos. Mag. 87 (2007) p.4421.
[28] B. Li and E. Ma, Phys. Rev. Lett. 103 (2009).
[29] X.Y. Zhang, B. Li, X.L. Wu, Y.T. Zhu, Q. Ma, Q. Liu, P.T. Wang and M.F. Horstemeyer, Scr. Mater. 67 (2012) p.862.
[30] S. Sandlöbes, M. Friák, S. Zaefferer, A. Dick, S. Yi, D. Letzig, Z. Pei, L.F. Zhu, J. Neugebauer and D. Raabe, Acta Mater. 60 (2012) p.3011.